Open Access

Catalysis Research

LIDSEN Publishing Inc.

Research Article

Effective $Cu/ZnO/Al_2O_3$ Catalyst for Methanol Production: Synthesis, Activation, Catalytic Performance, and Regeneration

Mikhail Kipnis [1, *], Elvira Volnina [1], Igor Belostotsky [1], Roman Galkin [1], Natalya Zhilyaeva [1], Ivan Levin [1], Sergey Kottsov [2, 3], Alexander Ezhov [1, 4]

1. Topchiev Institute of Petrochemical Synthesis, Russian Academy of Sciences, 119991, Moscow, Russia; E-Mails: kipnis@ips.ac.ru; volnina@ips.ac.ru; belostotsky@ips.ac.ru; galkinrs@yandex.ru; zhilyaeva@ips.ac.ru; levin@ips.ac.ru; alexander-ezhov@yandex.ru
2. Lomonosov Moscow State University, Faculty of Material Science, Leninskie gory 1, building 73, 119991, Moscow, Russia; E-Mail: sergey12-17@yandex.ru
3. Kurnakov Institute of General and Inorganic Chemistry, Leninsky Prospekt, 31, 119991, Moscow, Russia
4. Lomonosov Moscow State University, Faculty of Physics, Leninskie gory 1, building 2, 119991, Moscow, Russia

* **Correspondence:** Mikhail Kipnis; E-Mail: kipnis@ips.ac.ru

Academic Editor: Manashi Nath

Special Issue: Transition-Metal Based Catalysts for Clean Energy Conversion and Storage

Catalysis Research
2022, volume 2, issue 3
doi:10.21926/cr.2203027

Received: September 09, 2021
Accepted: September 06, 2022
Published: September 19, 2022

Abstract

A precursor $CuO/ZnO/Al_2O_3$ catalyst for methanol synthesis has been prepared at room temperature by introducing a ternary salt solution into the excess of sodium carbonate solution following the reverse co-precipitation method. The catalyst was tested for the synthesis of methanol from synthesis gas. The composition (vol. %) has been presented: CO, 22; CO_2, 5.8; N_2, 5.5; H_2, balance. The methanol productivity was recorded to be 2.7 kg kg_{cat}^{-1} h^{-1} at a temperature of 260 °C, a pressure of 3 MPa, and a space velocity of 61,700 l $(kg_{cat})^{-1}$ h^{-1}. The possibility of regenerating the activity of a catalyst subjected to conditions of artificial aging (overheating in a syngas environment) has been tested: approximately 92% of

the initial activity could be restored. Physicochemical studies were conducted using the thermogravimetric analysis (TGA), Fourier-transform infrared spectroscopy (FTIR), the scanning electron microscopy (SEM), and the X-ray diffraction (XRD) techniques using the Cu, Zn, and Al oxides obtained following the co-precipitation method. X-ray studies revealed that an amorphous phase was obtained from the Al oxide that was synthesized following both the direct and reverse co-precipitation methods. The calcination temperature was 300 °C. Individual oxides of Cu and Zn obtained following the reverse co-precipitation method form crystalline phases when calcined at 300 °C. When all three ingredients are present, calcination of the sample at 300 °C helps obtain an X-ray amorphous structure of the catalyst characterized by a high specific surface area. High-temperature carbonates are formed from samples prepared using a ternary mixture of nitrate salts when these are calcined at 300 °C.

Keywords
$Cu/ZnO/Al_2O_3$ catalyst; co-precipitation; methanol synthesis; methanol productivity; redox regeneration

1. Introduction

The demand for methanol is constantly growing. However, the increasing demand for methanol can be attributed to the fact that methanol is used for the synthesis of a number of compounds and the production of energy [1, 2].

Industrial synthesis of methanol is carried out from a mixture of H_2, CO, and CO_2 (synthesis gas), at a temperature in the range of 240–260 °C and pressure in the range of 5–10 MPa [3]. The primary reactions occurring during the synthesis of methanol involve the hydrogenation of CO_2 and CO to methanol and the water gas shift reaction. All reactions are exothermic and reversible. An effective low-temperature methanol catalyst based on the oxides of CuO, ZnO, and Al_2O_3 was developed in the 1960s [4]. However, it is still the most used industrial catalyst [5]. However, various aspects of the synthesis and operation of copper-containing catalysts are still under study [6].

A detailed study of the effect of pH and temperature on the properties of $CuO/ZnO/Al_2O_3$-based methanol catalysts prepared following the precipitation method using sodium carbonate and nitrate salts was carried out [7]. The positive effect of the increase in the precipitation temperature (70 °C) was noted. The promoting effect of the high-temperature conditions was ascribed to the uniform distribution of the components in the precipitate. The co-precipitation of Cu, Zn, and Al from nitrate and formate salts with sodium carbonate was studied [8] in an automated reactor. The reaction was carried out at 65 °C at a pH of 6.5. It is proposed that the micro-droplet precipitation technique or the method of precipitation from formate salts can help achieve a homogeneous distribution of components in the precipitate. For example, the co-precipitation of Cu and Zn using sodium carbonate (from nitrate salts) was also carried out at a pH of 6.5 and a temperature of 65 °C in an automated reactor [9]. The influence of a number of factors on the activity of the catalysts synthesized following the co-precipitation method was

considered in [10]. However, unlike the results reported in [8, 9], the authors reported that the higher the pH during the co-precipitation process (up to 9.2), the better the catalytic activity.

Numerous researchers have used the method of reverse co-precipitation, which involves introducing a solution of the corresponding nitrate salts into the precipitant. This helps achieve the simultaneous deposition of different cations.

In [11], the synthesis of an Al_2O_3/Cu/ZnO-based catalyst following the sequential precipitation method was proposed for the direct production of dimethyl ether (DME) from synthesis gas. Al nitrate was precipitated on the preformed Cu, Zn precipitate (an aqueous solution of metal nitrates was added drop-wise to a solution of $NaHCO_3$ at a pH of 6.6 at 70 °C).

Cu-ZnO/ZrO_2 catalysts were prepared following the reverse co-precipitation method under the influence of the ultrasound irradiation [12, 13]. Aqueous solutions of precursors were added drop-wise to a solution of $NaHCO_3$ (0.1 M) kept in an ultrasound bath operating in the temperature range of 37–47 °C under conditions of vigorous stirring. The pH of the precipitating solution was maintained in the range of 7.0–7.5 by continuously adding a solution of $NaHCO_3$ (0.1 M). In [14], the co-precipitation of Cu and Zn nitrates by Na carbonate at 65 °C was studied. Two options were considered: simultaneous mixing of the solutions at a constant pH and the introduction of a solution of Cu and Zn nitrates into a sodium carbonate solution at a decreasing pH method. It was noted that in the second variant, basic copper nitrate (gerhardtite) was present in the precipitate.

An increase in the precipitation temperature promotes an increase in the particle size [15], and high activity is achieved for catalysts obtained from precursors synthesized at temperatures ≤40 °C.

It is generally accepted that the presence of nitrate groups in Cu–Zn-containing precursors results in the sintering of copper oxide crystallites during heat treatment [4]. Hence, the synthesis must be carried out, preventing nitrate preservation in the precipitate. Analysis of the individual titration curves of Cu, Zn, and Al nitrates and the IR spectroscopic characteristics of the resulting precipitates revealed that precipitation with sodium carbonate at a pH of approximately 8 results in the formation of nitrates in the precipitate ([16], Figure S1, Figure S2, Table S1, Additional Materials). The method used by us [16] (where the method of reverse co-precipitation is conducted with an excess of sodium carbonate) makes it possible to obtain an efficient catalyst for the synthesis of methanol. It was observed that the fabricated catalyst was not inferior in activity to an industrial catalyst. The precipitation technique used was simple, and the execution of the method did not require the use of special equipment. Herein, we further our research on the catalyst obtained following the mentioned method.

A significant problem associated with Cu-containing catalysts used for methanol synthesis is the fact that the activity of the catalysts decreases gradually with time [17, 18]. In the absence of harmful impurities in the feedstock, the cause of the deactivation of copper catalysts can be attributed to carbon deposition or agglomeration of copper crystallites caused by the mobility of copper atoms at the reaction temperature [19].

In connection with studies of bifunctional catalysts for processing synthesis gas into various chemicals, there is an urgent interest in the problems of methanol catalyst regeneration [20-25]. The possibility of redox regeneration of a deactivated bifunctional CuO-ZnO-Al_2O_3/γ-Al_2O_3 catalyst for the synthesis of DME was demonstrated [26].

We studied a number of aspects of a methanol catalyst prepared following the reverse co-precipitation method. The methods of synthesis, the physicochemical characteristics, the activation of the catalyst under conditions of reduction treatment, the performance of the

synthesized catalyst, and the redox regeneration property of a catalyst directly subjected to conditions of preliminary aging under conditions of increased temperature in the presence of synthesis gas were explored.

2. Materials and Methods

2.1 Sample Preparation

The samples were synthesized using solutions of $Cu(NO_3)_2 \times 3H_2O$, $Zn(NO_3)_2 \times 6H_2O$, $Al(NO_3)_3 \times 9H_2O$, and Na_2CO_3 (reagents produced by JSC Lenreaktiv, Russia). The solutions were prepared using distilled water. Nitrates (0.2 mol/L) and sodium carbonate (0.3 mol/L) were used. The precipitation was carried out at room temperature. A pH meter (Akvilon 40, Akvilon Research and Production Company, Russia) was used to control the extent of precipitation. A number of samples were prepared for physicochemical studies in addition to the catalyst synthesized following the reverse co-precipitation method.

2.1.1 Syntheses following the Reverse Co-precipitation Method

Three-component sample. Individual solutions of nitrate salts of Cu (115 ml), Zn (57.5 ml), and Al (20 ml) were mixed, and the mixture was constantly stirred. The mixture was slowly added to a solution of Na_2CO_3 (196 mL). The pH decreased to 7.37 upon the addition of the nitrate solution. The solution with the precipitate was stirred for 3 h following the completion of precipitation. The pH increased to 8.97 under this condition. The solution with the precipitate was allowed to stand overnight at room temperature. The next day, the precipitate was filtered off, rinsed several times with cold water to neutral pH, dried at a temperature of 80 °C (overnight), and calcined in a muffle furnace under a flow of air at 300 °C (time: 5 h).

Synthesis of individual oxides of aluminum, copper, and zinc. During the synthesis of an Al-oxide sample, 133 mL of an aluminum nitrate solution was added to 163 mL of Na_2CO_3 solution. The pH decreased to 7.03 upon completion of the addition of the nitrate solution but increased to 7.55 after 2 h of stirring. The pH increased to 8.44 after overnight exposure. Sodium carbonate solution (110 mL) and copper nitrate solution (100 mL) were used for the synthesis of individual copper oxide samples. The volumes were 126 mL and 125 ml, respectively, for the synthesis of individual zinc oxide samples. The pH obtained after overnight exposure was 8.26 for copper and 7.85 for zinc. Subsequent operations were carried out with the resulting solutions containing precipitates, and the method of preparation was similar to the method used for the synthesis of the three-component sample under conditions of reverse co-precipitation.

Synthesis of double oxide CuO/ZnO. A mixed solution of Cu and Zn nitrates (2:1 ratio; 86.2 mL) was added to 86 mL of a Na_2CO_3 solution. The pH dropped to 8.86 and increased to 9.17 following aging and overnight exposure, respectively. Subsequent operations with the resulting solution containing the precipitate were carried out, and the methods were similar to the method used for the preparation of the three-component sample under conditions of reverse co-precipitation.

2.1.2 Syntheses under Conditions of Direct Co-precipitation

Three-component sample. Individual solutions of nitrate salts of Cu (115 mL), Zn (57.5 mL), and Al (20 mL) were mixed, and 196 mL of a sodium carbonate solution was slowly added to the

resulting solution. Upon mixing, the pH of the solution increased to 10.23. The solution containing the precipitate was stirred for 2 h following the cessation of the precipitation. Under these conditions, the pH of the solution decreased to 10.07. Subsequent operations with the resulting solution containing the precipitate were carried out following the methods used for the synthesis of a three-component sample (under conditions of reverse co-precipitation).

Synthesis of aluminum oxide. A solution of sodium carbonate (163 mL) was slowly added to a solution of aluminum nitrate (133 mL) under the conditions of stirring. The pH of the solution increased to 8.1 under these conditions. The solution containing the precipitate was stirred for 2 h following the cessation of precipitation. Under these conditions, a slight increase in the pH of the solution to 8.17 was observed. Subsequent operations with the resulting solution containing the precipitate were carried out following the process used for the synthesis of a three-component sample (under conditions of reverse co-precipitation).

2.2 Characterization Methods

The elemental analysis was carried out using the ARL™ PERFORM'X Sequential X-ray Fluorescence Spectrometer (Thermo Fisher Scientific, Switzerland).

The X-ray diffraction (XRD) technique was used for sample analysis, and the experiments were carried out using a Rigaku Rotaflex RU-200 diffractometer (Rigaku, Japan; radiation: CuKα). The crystallite sizes were studied using the Scherrer formula by analyzing the broadening of the main peak [27].

The specific surface of the samples and their porosity were determined using a Micromeritics ASAP 2020 instrument (USA) under conditions of capillary adsorption of nitrogen at 77 K.

The specific surface of the samples was calculated following the Brunauer–Emmett–Teller (BET) method, and the volume and average pore size were calculated using the Barret–Joyner–Halenda (BHJ) method using the Micromeritics software. The process of preliminary degassing of the samples was carried out at a temperature of 300 °C over a period of 1 h.

The morphological features of the samples were studied using the scanning electron microscopy (SEM) technique. The X-ray energy dispersive analysis (EDX) technique determined the local elemental composition. The Cu-containing samples were analyzed using the SEM and EDX techniques using a Carl Zeiss NVision 40 CrossBeam microscope equipped with an Oxford Instruments X-Max analyzer. The accelerating voltage was maintained at 5 kV while using the SEM technique, and it was 20 kV when the EDX method was used. Standard secondary-electron (SE), in-lens SE, and energy selective backscattered (EsB) electron detectors were used for SEM studies. The EDX results were obtained for six regions of each sample.

The SEM images of the Al oxide samples were obtained using a Phenom XL microscope (Thermo Fisher Scientific, USA), and the accelerating voltage was maintained at 15.0 kV.

The thermogravimetric analysis (TGA) technique was used under conditions of differential scanning calorimetry. The DSC823e instrument (Mettler Toledo, USA) was used, and the experiments were conducted in air (heating rate: 10 K/min).

IR spectra were recorded under the reflection mode on an IFS-66 v/s Bruker IR Fourier spectrometer (15 scans, ZnSe crystal, range 600–4000 cm^{-1}).

2.3 Catalytic Performance Tests

Catalytic experiments were carried out following the setup presented in [28]. The conventional fixed bed flow reactor is made of stainless steel (internal diameter: 12 mm). A thermocouple channel (outer diameter: 6 mm) is located along the axis of the reactor. A table with a metal mesh is placed on the thermocouple channel to accommodate a weighed portion of the catalyst. The reactor was heated using an electric furnace. The temperature at the inlet and outlet of the catalyst bed was controlled by two thermocouples located at appropriate levels of the thermocouple channel.

Samples for testing were prepared by mixing powders (size of the fraction: <0.1 mm) of catalyst and quartz in a ratio of 1/1 (by weight). Following this, the samples were pressed on an RP-12 hand press (Biolent, Russia). A colloidal graphite additive (~1 wt.%) was introduced into the charge mixture before pelletizing to achieve high compressibility. The resulting pellets with a height of ~1 mm were crushed to a fraction, the size of which was in the range of 0.4–0.63 mm. A 0.8 g sample was used for the experiments.

The stream of the hot converted gas at the outlet of the reactor was divided into two parts by a set of valves. The analyzed flow was directed to a heated chromatograph line (Kristall 5000, Khromatek, Russia), and the main flow was directed to a condenser to separate the liquid fraction. The release was achieved via a back-pressure controller. The reactor outlet and the corresponding gas lines under pressure were maintained at a temperature of ≥120 °C. An additional heater was used for heating.

Synthesis gas (composition, vol.%: CO, 22; CO_2, 5.8; N_2, 5.5; H_2, balance) was prepared from individual gases in the preliminarily evacuated cylinder. The pressure was controlled by taking readings from a digital sensor calibrated by a standard pressure gauge.

The flow rate of the converted gas at the outlet of the reactor was calculated based on the material balance of nitrogen. Chromatographic analysis was performed using three independent lines and thermal conductivity detectors [29]. The contents of CO_2, DME, water, and methanol were determined on the line with a packed column with porapak T. Helium was used as the carrier gas. The contents of N_2 and CO were determined on the line with a packed column containing zeolite NaX. Helium was used as the carrier gas. Likewise, the H_2 content was determined on the line with a packed column with NaX zeolite. In this case, argon was used as the carrier gas. The maximum error in determining the concentrations of the components was in the range of 5–7 rel.%, and the maximum error for the flow rates was in the range of 1–3 rel.%. As a rule, the maximum error in carbon balance was 5 rel.%. The temperature in the reactor was maintained with an error of no more than 1 °C, and for the pressure, the error was no more than 0.02 MPa. Data for gas volumes are presented at standard temperature and pressure (STP), that is, 0 °C and 0.1 MPa.

The catalyst was activated to reduce copper oxide using a mixture of ≈ 2.4 vol.% of H_2/N_2 (flow rate: 2 Nl/h). The temperature was increased to 200 °C at a rate of approximately 0.5 °C/min, and this was achieved by controlling the chromatographic absorption of H_2 and the release of H_2O. Post activation, the catalyst was left overnight in the same mixture at a temperature of 260 °C and pressure in the range of 0.2–0.3 MPa to reduce the time for preparatory procedures. The next day, synthesis gas was fed into the reactor (pressure: ≤3 MPa), and the corresponding experiments

were carried out. When the catalyst was preserved overnight or over weekends, the synthesis gas was replaced with a mixture of H_2/N_2 or H_2 at reduced pressure (range: 0.2–0.3 MPa).

The possibility of catalyst regeneration was studied. The catalyst was artificially aged under overheated conditions in a syngas environment at a temperature of >300 °C. The pressure was maintained at 3 MPa. The aged catalyst was then cooled to approximately 70 °C under a flow of nitrogen and oxidized in a 1% O_2/N_2 mixture. The temperature was slowly raised until oxygen uptake ceased. Following this, the usual procedure for catalyst activation was carried out.

2.4 Calculation Formulae

The flow rate of the converted gas in the reactor (V_{out}, Nl/h) was calculated based on the material balance for nitrogen. The following formula was used:

$$V_{out} = V_{in}C_{in}/C_{out}, \quad (1)$$

where C_{in} and C_{out} are the nitrogen concentrations at the inlet and outlet of the reactor, respectively, and V_{in} is the gas flow rate at the inlet of the reactor (Nl/h).

CO conversion (Xco, %) was calculated based on the values of the gas flow rates at the inlet and outlet from the reactor as follows:

$$X_{CO} = (C_{in}V_{in} - C_{CO}V_{out}) \times 100/(C_{in}V_{in}), \quad (2)$$

where C_{in} and C_{CO} are the CO concentrations in the feed and converted gas, respectively.

The space-time yield or productivity of the catalyst with respect to the oxygenates (methanol and DME) was calculated based on methanol content (P, g_{met} kg_{cat}^{-1} h^{-1}) as follows:

$$P = 32V_{out}(2C_D + C_M)(22.4 \times m \times 100)^{-1}, \quad (3)$$

where 32 indicates the molar mass of methanol, m is the weight of the catalyst, and C_D and C_M are the DME and methanol concentrations in the converted gas, respectively.

3. Results and Discussion

3.1 Characterization of the Samples

3.1.1 X-ray Phase Analysis and Sample Porosity

The characteristics of the porous structure of the samples prepared following the reverse co-precipitation method are presented in Table 1, and the diffraction patterns are presented in Figure 1.

Table 1 Characteristics of the porous structure of the calcined (300 °C) samples prepared following the reverse precipitation method.

Designation of the sample	Composition*	Specific surface area BET, m^2/g	Pore volume cm^3/g	Average pore size BET, nm
Al	Al_2O_3	210.7	1.03	19.9
Zn	ZnO	53.9	0.43	32.4
Cu	CuO	42.9	0.23	21.7
Cu/Zn/Al	$6CuO/3ZnO/Al_2O_3$	112.5	0.40	14.5
Cu/Zn	2CuO/ZnO	49.5	0.21	21.4

* Based on metal oxides

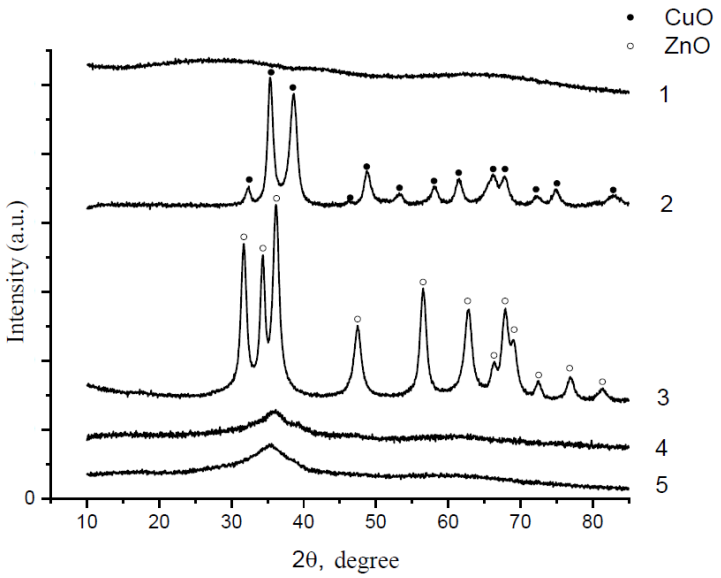

Figure 1 Diffraction patterns recorded for the samples prepared following the reverse precipitation method (calcination at 300 °C). *1 – Al*, *2 – Cu*, *3 – Zn*, *4 – Cu/Zn/Al*, *5 – Cu/Zn*.

The precipitated aluminum hydroxide sample after calcination at 300 °C is X-ray amorphous (Figure 1, curve *1*). Similar observations were made for the aluminum oxide sample obtained following the process of direct precipitation (Figure S3, Additional Materials). When the sample was further calcined at 450 °C for 6 h, the shape of the diffractogram was not changed.

The precipitates of individual Cu and Zn salts calcined at 300 °C were well-crystallized oxides (Figure 1, curves *2*, *3*) of crystallite sizes 12 and 10 nm, respectively. They were identified as tenorite (JCPDS-ICDD PDF file #48–1548) and zincite (JCPDS-ICDD PDF file #36–1451). For the case of the Cu–Zn–Al system, only the X-ray amorphous phase could be identified following calcination at 300 °C (Figure 1, curve *4*). For the case of the binary *Cu/Zn* sample, only the X-ray amorphous phase was identified (Figure 1, curve *5*). In both cases, a wide halo was observed in the diffraction patterns in the range of angles corresponding to the angular positions of the main peaks corresponding to the copper and zinc oxide phases. Thus, the simultaneous co-precipitation of salts helps disperse the resulting oxides.

Analysis of the adsorption–desorption isotherms of the samples (Figure S4, Additional Materials) made it possible to determine the characteristics of the porous structure. The specific pore volume in individual samples differs significantly (Table 1). The maximum pore volume was recorded for the *Al* sample (1.03 cm^3/g), and the minimum pore volume was recorded for the *Cu* sample (0.23 cm^3/g). The maximum specific surface area was also recorded for the *Al* sample (210.7 m^2/g), and the minimum value was recorded for the *Cu* sample (42.9 m^2/g). In a binary *Cu/Zn* sample, the specific volume and average pore size are practically the same as those in the *Cu* sample, and the specific surface area is between the corresponding values of individual samples. The situation changes significantly in the case of a ternary sample. A decrease in the average pore size and a noticeable increase in the specific surface area are observed under these conditions. Thus, it can be concluded that during the synthesis of the catalyst, the co-precipitating compounds (copper-, zinc-, and aluminum-based compounds) do not tend to form large pores in the precipitate, which results in an increase in the specific surface area of the catalyst.

3.1.2 Morphology and Elemental Analysis of Samples (Syntheses by Reverse Co-precipitation)

During the synthesis of the catalyst, the calculated ratio of the initial metal salts was chosen based on the calcined sample (CuO: 60 wt.%; ZnO: 30 wt.%; Al_2O_3: 10 wt.%; in terms of moles: CuO: 0.62; ZnO: 0.30; Al_2O_3: 0.08). The synthesis process was repeated multiple times, and it was observed that according to the elemental analysis data (error no worse than 5% rel.), the content of copper and zinc oxides remains the same, while the content of aluminum oxide for different samples was in the range of 6–10 wt.%. The content of metals is insignificant in the mother liquor during synthesis [16]. The reduction in the content of alumina in the samples can be potentially attributed to the partial entrainment of the highly dispersed aluminum compounds particles during filtration and washing.

The typical EDS spectra of copper-containing samples (Table 1) are shown in Figure S5, Figure S6, and Figure S7 (Additional Materials). The calculated ratio in at.% for a three-component Cu/Zn/Al sample was 1/0.49/0.26. According to the analysis of the EDS spectra of the sample, the ratio is usually 1/0.56/0.02 (the standard deviation for the Zn/Cu ratio is 0.14, and that for the Al/Cu ratio is 0.004). Repeated synthesis of the sample was achieved, and the ratio was determined to be 1/0.49/0.19 for the repeatedly synthesized sample (the standard deviations for Zn/Cu and Al/Cu were the same and was equal to 0.01). In both cases, the Cu/Zn ratio was close to the calculated one, while the Al/Cu ratio was underestimated. We believe that this can be explained by the partial entrainment of the aluminum oxide during synthesis.

For a two-component *Cu/Zn* sample, the calculated ratio in at.% was determined to be 1/0.5. According to the analysis of the EDS spectra, the actual ratio was 1/0.52 (standard deviation: 0.02), and this value agrees well with the calculated ratio.

Let us compare the EDS spectrum of the *Cu/Zn* sample with the spectrum of *Cu* (Figure S6 and Figure S7, Additional Materials). It can be seen that the spectral profiles of the *Cu/Zn* and *Cu* samples in the region of 1.2–1.8 keV, where a peak characteristic of Al is observed, are similar. However, the assignment of the weak peak in the spectrum recorded for the Cu/Zn sample to aluminum can be attributed to instrumental error.

Morphological features of the samples are presented in a number of images (Figures S8–S11, Additional Materials). The *Cu/Zn/Al* sample contains “blocks” of different sizes (Figure S8).

Granules and pores of sizes in the 10–20 nm range were observed. A scale of 100 nm was used to distinguish lamellar particles. The Cu/Zn sample consists of "blocks" of various sizes. The "blocks" are not rounded. No pronounced pores (on the scale of hundreds and tens of nanometers) are observed on the surface of the particles (Figure S9). Granules in size range of 20–30 nm are the characteristic features of the samples. The Cu sample primarily consists of spherical particles of diameters in the range of 5–20 microns. These contain cubic particles of the size of approximately 100 nm (Figure S10).

The Al oxide samples (regardless of the precipitation method used), when calcined at 300 °C, contain well-faceted particles in the size range of tens to hundreds of microns (Figure S11, Additional Materials).

3.1.3 Thermogravimetric Analysis

The TGA data corresponding to the calcined three-component samples containing oxides of Cu, Zn, and Al, synthesized following the reverse and direct precipitation methods, are presented in Figures S12–S13 (Additional Materials). When heated to 1000 °C, the total weight loss of the samples was 13.5 wt.% (reverse co-precipitation) and 14.7 wt.% (direct co-precipitation). Weight loss intervals can be distinguished: four intervals for the sample synthesized by reverse co-precipitation and three intervals for the sample synthesized by direct co-precipitation. Weight loss occurring till the temperature of 300 °C can be associated with the loss of adsorbed water and CO_2 and, possibly, the decomposition of residual hydroxocarbonates [30]. Therefore, we plan to optimize the conditions for the calcination of the resulting precipitate in the future. High-temperature weight loss was noted [30] (700–900 K) for the methanol catalyst precursor synthesized following the direct co-precipitation method using sodium carbonate. According to physicochemical studies, this weight loss is associated with the decomposition of the high-temperature carbonate samples formed during precipitation [30]. The observed temperature maxima appearing in the DTG curve (at temperatures above 300 °C) are ascribed to the decomposition of high-temperature carbonates.

High-temperature mass loss peak was not observed in the TGA profile recorded for the *Cu* sample. Thus, high-temperature carbonate is not directly related to copper and is characteristic of a three-way catalyst.

3.1.4 IR Spectroscopic Studies

Figure S14 (Additional Materials) shows the IR spectra of the three-component samples ($CuO/ZnO/Al_2O_3$) synthesized following reverse (1) and direct (2) co-precipitation methods. The process was followed by the process of calcination at 300 °C. Although the samples were synthesized differently, similar spectra were obtained.

Bands appearing at 1482.3, 1399.7, and 840.1 cm^{-1} can be attributed to the carbonate ions [31]. The wide halo in the region of 3600–3000 cm^{-1} is associated with the presence of hydroxyl groups of adsorbed water.

3.2 *Methanol Productivity and CO Conversion*

During the activation of the catalyst, starting from approximately 150 °C, the absorption of H_2 and the release of the resulting water molecules are observed (Figure S15, Additional Materials). The maximum hydrogen uptake corresponds to the maximal water evolution. Reduction ends at ~200 °C. The total H_2 uptake corresponds to the reduction of the copper oxide contained in the catalyst. Thus, the complete reduction of copper oxide under rather "mild" conditions can be achieved if the H_2 and H_2O contents are controlled at the outlet of the reactor during the process of catalyst activation.

The behavior of the catalyst with varying space velocity is shown in Figure 2.

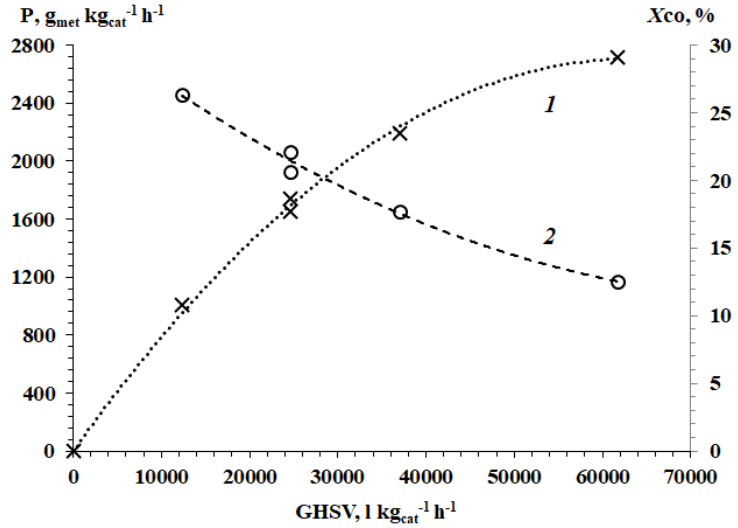

Figure 2 Dependence of the productivity of the catalyst (*1*) and the conversion of CO (*2*) during the synthesis of methanol on the space velocity.

As expected, the conversion of CO (*X*co) monotonically decreases with an increase in space velocity. So, at GHSV 12,300 l kg_{cat}^{-1} h^{-1}, it was 26%, and at 61,700 l kg_{cat}^{-1} h^{-1} it was 12.5%. With an increase in the volumetric velocity, the yield of methanol (productivity) increases to a certain limit (Figure 2). The curve presenting the dependence of productivity on the space velocity reflects a gradual transition from the region depending on the equilibrium conditions of methanol synthesis to the kinetic region [32].

In addition to methanol, the products contain an insignificant amount of DME, which is formed during methanol dehydration, a side reaction. Its content does not exceed 0.15 vol.% at GHSV 12,300 l kg_{cat}^{-1} h^{-1}, and the content decreases with increasing GHSV.

The data series shown in Figure 2 was received during the working day. The series started and ended at the space velocity 24,700 l kg_{cat}^{-1} h^{-1}. The maximum productivity in terms of methanol, achieved with an increase in the GHSV to 61,700 l kg_{cat}^{-1} h^{-1}, was 2.7 kg kg_{cat}^{-1} h^{-1}. According to [16], the productivity of the synthesized catalyst exceeds the productivity of a commercial catalyst: 2 kg kg_{cat}^{-1} h^{-1} against 1.8 kg kg_{cat}^{-1} h^{-1} when the space velocity was 31,000 l kg_{cat}^{-1} h^{-1}. Authors [4] note that the productivity achieved using a typical industrial $Cu/ZnO/Al_2O_3$ catalyst operated at 250 °C (pressure: 5 MPa; space velocity: 10,000 h^{-1}) during methanol synthesis was 71.4 mol l_{kat}^{-1} h^{-1} or 2.28 kg l_{cat}^{-1} h^{-1}.

The overheating of the catalyst bed corresponding, caused by the exothermicity of the methanol synthesis reaction, correlates with productivity (Figure 3).

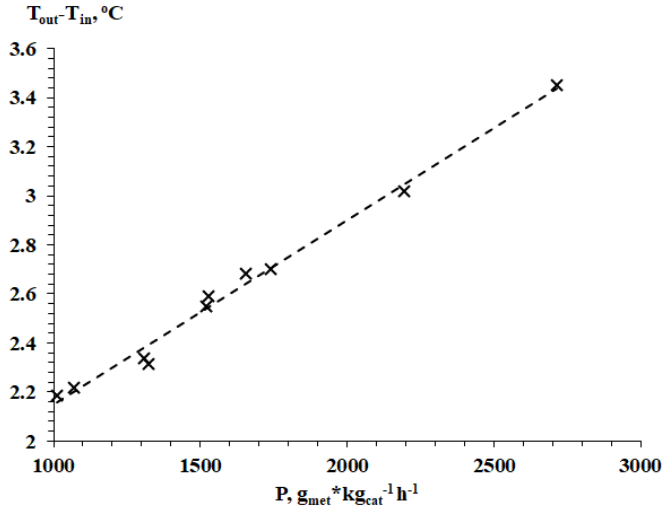

Figure 3 Correlation of the overheating of the catalyst bed with the productivity of the catalyst during methanol synthesis.

In this case, the trend line is described by the following relation:

$(T_{out}-T_{in}) = 0.001*P + 1.4$.

The constant practically coincides with the temperature difference between the inlet and outlet from the layer in the absence of a reaction (weighed portion-aluminum oxide; 1.3 °C).

3.3 Influence of the Nature of the Catalyst Treatment Method on the Activity of the Catalyst

Several different catalyst treatment methods, including the redox regeneration method (Section 3.4), were used . After each treatment cycle, the catalytic activity was determined under standardized conditions (260 °C, 3 MPa, GHSV 24,700 l kg_{cat}^{-1} h^{-1}).

Runs were conducted at 260 °C under conditions of varying GHSV. Following this, the catalyst was cooled to 240 °C, and the synthesis gas was replaced with a mixture of H_2/N_2. Subsequently, the sample was held for 64 h under a pressure of 0.3 MPa. The mixture was replaced with synthesis gas, the pressure was raised to 3 MPa, and the temperature was increased to 260 °C. Under these conditions, the activity was checked. There was a slight decrease in performance compared to the first day of operation, but the catalyst ran stably for 3.5 h.

The corresponding data on the activity of the catalyst are presented in Table 2.

Table 2 Influence of the nature of the treatment method on the activity of the catalyst. Working conditions: 260 °C, 3 MPa, GHSV 24,700 l kg_{cat}^{-1} h^{-1}.

Operation	CH_3OH, vol.%	*X*co, %	P g_{met} kg_{cat}^{-1} h^{-1}	$P_{r,\%}$
Activation	5.3	22.1	1740	105
5.5 h of work	5.05	20.6	1655	100

240 °C, 64 h, mixture H_2/N_2	4.7	19.3	1526	92
334 °C, synthesis gas, 1 h	4.0	15.9	1325	80
First regeneration, activation	4.65	18.7	1520	92
397 °C, synthesis gas, 1 h	3.2	12.5	1070	65
Second regeneration, activation	3.95	15.9	1310	79

In addition to the data on methanol content, CO conversion, and methanol productivity, the relative productivity (P_r) was also evaluated. The data obtained at the end of the run on the first day are taken as 100% while calculating P_r. A slight decrease in the activity, both on the first day of operation and after a long exposure at 240 °C, indicates the running-in of the catalyst.

The catalyst was subjected to conditions of artificial aging. The temperature was maintained at 334 °C, and then, after regeneration at 397 °C. Conditions of forced aging reduced the activity of the system. When held at 334 °C, the relative productivity was recorded to be 80%. The productivity was recorded to be 65% when the samples were held at 397 °C. These results are consistent with previously reported data [22]. Thus, according to [22], with an increase in the temperature of the methanol synthesis reaction from 270 to 350 °C (operation for about 40 h), a decrease (by approximately 20–50%) is observed in the active surface of copper.

The regeneration process (Section 3.4) resulted in a noticeable restoration of activity, which indicates the success of the regeneration procedure.

3.4 Aging and Redox Catalyst Regeneration

The dynamics of the change in the oxygen content during the oxidation of the catalyst sintered at 334 °C are shown in Figure 4.

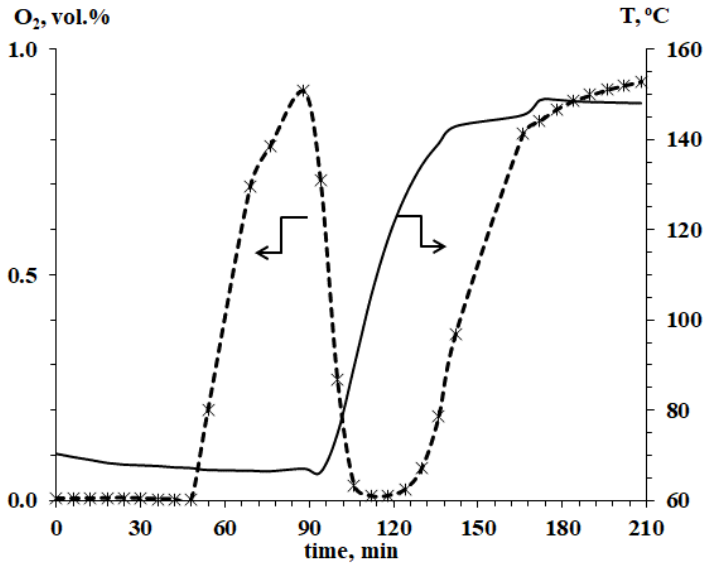

Figure 4 Dynamics of the oxygen content at the outlet during the oxidation of the catalyst subjected to sintering conditions at 334°C.

Oxygen was actively absorbed at approximately 70 °C (a 1% O_2/N_2 mixture was fed into the reactor) for approximately 50 min. Further, at the exit of the reactor, an increase in its content was observed, and the content was comparable to the initial value. The temperature rise resulted

in a decrease in the oxygen yield initially. Following this, the yield increased. Evaluation of the total amount of absorbed oxygen showed that it corresponds to the complete oxidation of copper contained in the reduced catalyst.

The dynamics of the oxidation process of metallic copper in a working catalyst can be explained. The surface of copper crystallites is easily oxidized at temperatures close to 70 °C, but the oxidation of the internal volume of copper crystallites is difficult, and this difficulty can be attributed to diffusion restrictions. Indeed, for the oxidation of copper atoms in the inner volume of the crystallite, diffusion of O_2 molecules into the volume and the diffusion of the resulting H_2O molecules outside are required. These processes are temperature-dependent. An increase in the temperature helps overcome diffusion limitations. Post oxidation, the usual procedure for activating the catalyst was carried out (Figure S15, Additional Materials).

3.5 Effect of Temperature on the Activity of Catalysts

The effect of temperature on the performance of the catalyst at a fixed volumetric velocity of 25,000 l kg_{cat}^{-1} h^{-1} was studied. The temperature, starting from 260 °C, was successively reduced to 180 °C (interval: 20 °C).

In this case, H_2 was used instead of the H_2/N_2 mixture during catalyst holding post activation. It was also used between tests at different temperatures. The activity of the new sample at 260 °C was comparable to the activity of the previous one: the initial methanol content was 5.5 (versus 5.3 vol.%). During the first 4.5 h of operation, a slow decrease in activity is observed, and this can be potentially attributed to the running-in of the catalyst.

Catalyst productivity as a function of temperature was studied to estimate the apparent activation energy of the methanol synthesis reaction (Figure 5).

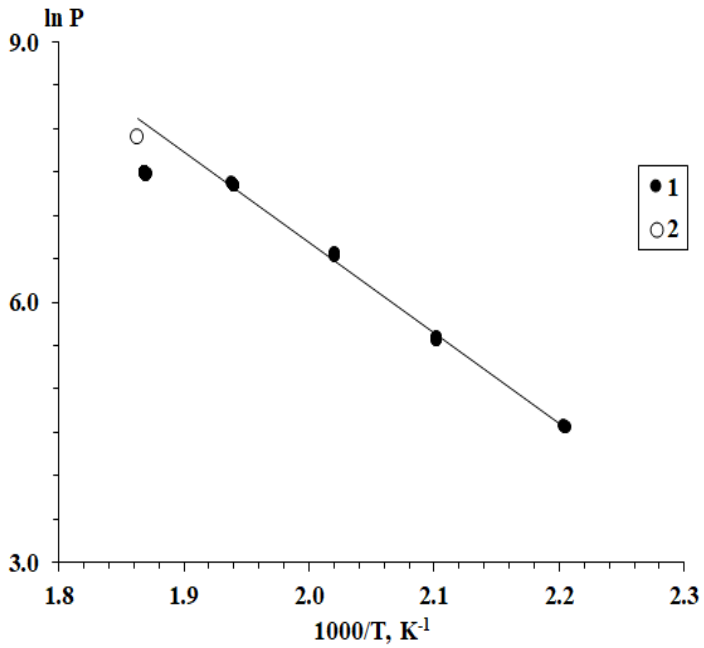

Figure 5 Arrhenius dependence of methanol synthesis productivity. Data for GHSV: 1 – 25,000 l kg_{cat}^{-1} h^{-1}, 2 – 61,700 l kg_{cat}^{-1} h^{-1}.

As can be seen from Figure 5, the data obtained at a temperature of 240 °C and below fit well with the linear equation presented when GHSV was 25,000 l kg_{cat}^{-1} h^{-1}.

A deviation in the value obtained at 260 °C was also observed. First, we analyzed the data on the influence of GHSV on the performance of the catalyst at 260°C (Figure 2). A catalyst is known to be under the kinetic mode when its performance is limited by its activity. When operating in this mode, an increase in the reactant supply does not result in an increase in productivity. As can be seen from Figure 2, at a GHSV of 25,000 l kg_{cat}^{-1} h^{-1}, the kinetic regime is not achieved. The use of the maximal load (GHSV = 61,700 l kg_{cat}^{-1} h^{-1}, Figure 2) suggests a better match of linearity (Figure 5; value 2). Based on Figure 5, it is possible to estimate the apparent activation energy of methanol synthesis (87 kJ/mol). The value is close to the previously reported value of 70 kJ/mol [3].

4. Conclusions

An effective $CuO/ZnO/Al_2O_3$-based methanol catalyst was synthesized at room temperature following the method of reverse co-precipitation. The method involved dropping a metal salt solution into a sodium carbonate solution. After aging, filtration, and heat treatment of the precipitate (calcined at 300 °C), the catalyst was characterized. Finely dispersed X-ray amorphous oxides of copper, zinc, and aluminum were observed. In addition, a developed specific surface area and a significant specific pore volume characterize the catalyst. The catalyst was tested for the synthesis of methanol from synthesis gas (composition, vol.%: CO, 22; CO_2, 5.8; N_2, 5.5; H_2, balance). The reaction temperature was maintained at 260 °C, and the pressure was maintained at 3 MPa. Under these conditions, the productivity of 2.7 kg kg_{cat}^{-1} h^{-1} was achieved, which corresponds to the performance of an industrial catalyst. The correlation between the heating of the catalyst bed and its productivity was studied. The apparent activation energy of the reaction resulting in methanol synthesis (in the temperature range of 180–260 °C) was 87 kJ/mol. The possibility of regeneration of a catalyst subjected to conditions of artificial aging (overheating above 300 °C in a syngas environment) has been tested by conducting sequential oxidation/reduction reactions. Successive oxidation of the aged catalyst in a 1% O_2/N_2 mixture at a temperature not higher than 150 °C and the activation of the catalyst results in the 92% (first regeneration) and 79% (second regeneration) restoration of the activity of the catalyst.

Acknowledgments

This work was performed using the equipment at the Shared Research Center «Analytical center of deep oil processing and petrochemistry of TIPS RAS» and the Center for collective use of Institute of Problems of Chemical Physics of the Russian Academy of Sciences «New Petrochemical Processes, Polymer Composites, and Adhesives».

Author Contributions

Mikhail Kipnis formulated research objectives, analyzed literature, supervised the work, and prepared the final version of the manuscript. Elvira Volnina developed a method for catalyst synthesis, synthesized samples, and contributed to the writing of the manuscript. Igor Belostotsky developed a methodology and analyzed the results of catalytic studies. Roman Galkin conducted experiments on activation, catalysis, catalyst regeneration and contributed to the writing of the

manuscript. Natalya Zhilyaeva conducted a study of the porous structure of the catalyst and contributed to the writing of the manuscript. Ivan Levin performed an X-ray analysis of samples and contributed to the writing of the manuscript. Sergey Kottsov and Alexander Ezhov performed an SEM and EDS analysis of samples and contributed to the writing of the manuscript.

Funding

This work was performed under a state task to Topchiev Institute of Petrochemical Synthesis of the Russian Academy of Sciences.

Competing Interests

The authors have declared that no competing interests exist.

Additional Materials

The following additional materials are uploaded at the page of this paper.

1. Figure S1: Titration curves corresponding to the individual nitrate solutions of Cu, Zn, and Al.
2. Table S1**:** Characteristics of the precipitates (dried at 80 °C) of the individual nitrates studied using the IR spectroscopy technique.
3. Figure S2: IR spectra of the precipitates of individual nitrates of Cu, Zn, and Al dried at 80°C (samples Table S1). a – Cu (*1*), Zn (*2*), b – Al.
4. Figure S3: Diffraction patterns of the synthesized Al samples (calcination at 300 °C). 1– reverse co-precipitation, 2–direct co-precipitation.
5. Figure S4: Adsorption–desorption isotherms recorded for the samples calcined at 300 °C: *a, b, c* – precipitated oxides Al, Zn, Cu, *d* – *Cu/Zn/Al* sample, *e* – *Cu/Zn* sample (Table 1).
6. Figure S5: EDS spectral profile recorded for the *Cu/Zn/Al* sample.
7. Figure S6: EDS spectral profile recorded for the *Cu/Zn* sample.
8. Figure S7: EDS spectral profile recorded for the *Cu* sample.
9. Figure S8: Morphology of the *Cu/Zn/Al* sample.
10. Figure S9: Morphology of the *Cu/Zn* sample.
11. Figure S10: Morphology of the *Cu* sample.
12. Figure S11: Morphology of the Al oxide samples synthesized following the reverse (*a*) and direct co-precipitation (*b*) methods (calcination temperature: 300 °C).
13. Figure S12: Results obtained using the thermogravimetry technique for a three-component sample ($CuO/ZnO/Al_2O_3$) synthesized following the reverse co-precipitation method (calcination temperature: 300 °C).
14. Figure S13: Results obtained using the thermogravimetry technique for a three-component sample ($CuO/ZnO/Al_2O_3$) synthesized following the direct co-precipitation method (calcination temperature: 300 °C).
15. Figure S14: IR spectral profiles recorded for the three-component samples ($CuO/ZnO/Al_2O_3$) synthesized following the reverse (1) and direct (2) co-precipitation method (calcination temperature: 300 °C).
16. Figure S15: Activation of the catalyst in a mixture of H_2/N_2 (2 Nl/h). *1*-H_2, *2*-H_2O.

References

1. Dalena F, Senatore A, Marino A, Gordano A, Basile M, Basile A. Chapter 1-Methanol production and applications: An overview. In: Methanol: Science and engineering. Amsterdam: Elsevier; 2018. pp. 3-28.
2. Bozzano G, Manenti F. Efficient methanol synthesis: Perspectives, technologies and optimization strategies. Prog Energy Combust Sci. 2016; 56: 71-105.
3. Kunkes E, Behrens M. Methanol chemistry. In: Chemical energy storage. Berlin: De Gruyter Textbook; 2013. pp. 413-442.
4. Chinchen GC, Denny PJ, Jennings JR, Spencer MS, Waugh KC. Synthesis of methanol: Part 1. Catalysts and kinetics. Appl Catal. 1988; 36: 1-65.
5. Zhong J, Yang X, Wu Z, Liang B, Huang Y, Zhang T. State of the art and perspectives in heterogeneous catalysis of CO_2 hydrogenation to methanol. Chem Soc Rev. 2020; 49: 1385-1413.
6. Dang S, Yang H, Gao P, Wang H, Li X, Wei W, et al. A review of research progress on heterogeneous catalysts for methanol synthesis from carbon dioxide hydrogenation. Catal Today. 2019; 330: 61-75.
7. Baltes C, Vukojević S, Schüth F. Correlations between synthesis, precursor, and catalyst structure and activity of a large set of $CuO/ZnO/Al_2O_3$ catalysts for methanol synthesis. J Catal. 2008; 258: 334-344.
8. Behrens M, Brennecke D, Girgsdies F, Kißner S, Trunschke A, Nasrudin N, et al. Understanding the complexity of a catalyst synthesis: Co-precipitation of mixed Cu,Zn,Al hydroxycarbonate precursors for $Cu/ZnO/Al_2O_3$ catalysts investigated by titration experiments. Appl Catal A Gen. 2011; 392: 93-102.
9. Schumann J, Tarasov A, Thomas N, Schlögl R, Behrens M. Cu,Zn-based catalysts for methanol synthesis: On the effect of calcination conditions and the part of residual carbonates. Appl Catal A Gen. 2016; 516: 117-126.
10. Kiener C, Kurtz M, Wilmer H, Hoffmann C, Schmidt HW, Grunwaldt JD, et al. High-throughput screening under demanding conditions: Cu/ZnO catalysts in high pressure methanol synthesis as an example. J Catal. 2003; 216: 110-119.
11. Jeong C, Ham H, Bae JW, Kang DC, Shin CH, Baik JH, et al. Facile structure tuning of a methanol-synthesis catalyst towards the direct synthesis of dimethyl ether from syngas. ChemCatChem. 2017; 9: 4484-4489.
12. Arena F, Italiano G, Barbera K, Bordiga S, Bonura G, Spadaro L, et al. Solid-state interactions, adsorption sites and functionality of $Cu\text{-}ZnO/ZrO_2$ catalysts in the CO_2 hydrogenation to CH_3OH. Appl Catal A Gen. 2008; 350: 16-23.
13. Arena F, Barbera K, Italiano G, Bonura G, Spadaro L, Frusteri F. Synthesis, characterization and activity pattern of $Cu–ZnO/ZrO_2$ catalysts in the hydrogenation of carbon dioxide to methanol. J Catal. 2007; 249: 185-194.
14. Bems B, Schur M, Dassenoy A, Junkes H, Herein D, Schlögl R. Relations between synthesis and microstructural properties of copper/zinc hydroxycarbonates. Chem Eur J. 2003; 9: 2039-2052.
15. Wu J, Luo S, Toyir J, Saito M, Takeuchi M, Watanabe T. Optimization of preparation conditions and improvement of stability of Cu/ZnO-based multicomponent catalysts for methanol synthesis from CO_2 and H_2. Catal Today. 1998; 45: 215-220.

16. Kipnis MA, Volnina EA, Belostotskii IA, Levin IS. Features of preparation of the methanol synthesis component of a bifunctional dimethyl ether synthesis catalyst. Kinet Catal. 2020; 61: 145-154.
17. Hirotani K, Nakamura H, Shoji K. Optimum catalytic reactor design for methanol synthesis with TEC MRF-Z® reactor. Catal Surv Asia. 1998; 2: 99-106.
18. Fichtl MB, Schlereth D, Jacobsen N, Kasatkin I, Schumann J, Behrens M, et al. Kinetics of deactivation on $Cu/ZnO/Al_2O_3$ methanol synthesis catalysts. Appl Catal A Gen. 2015; 502: 262-270.
19. Riaz A, Zahedi G, Klemeš JJ. A review of cleaner production methods for the manufacture of methanol. J Clean Prod. 2013; 57: 19-37.
20. Lu P, Hondo E, Chizema LG, Lu C, Mei Y, Tong M, et al. Influence of tandem catalysis and optimised parameters on syngas-dimethyl ether co-fed process for ethanol direct synthesis in a dual bed reactor. Catal Lett. 2019; 149: 3203-3216.
21. Feng X, Yao J, Zeng Y, Cui Y, Kazumi S, Prasert R, et al. More efficient ethanol synthesis from dimethyl ether and syngas over the combined nano-sized ZSM-35 zeolite with CuZnAl catalyst. Catal Today. 2021; 369: 88-94.
22. Lorenz E, Wehling P, Schlereth M, Kraushaar-Czarnetzki B. Influence of the spatial arrangement of catalyst components in the single-stage conversion of synthesis gas to gasoline. Catal Today. 2016; 275: 183-190.
23. Masudi A, Jusoh NWC, Muraza O. Recent progress on low rank coal conversion to dimethyl ether as clean fuel: A critical review. J Clean Prod. 2020; 277: 124024.
24. Saravanan K, Ham H, Tsubaki N, Bae JW. Recent progress for direct synthesis of dimethyl ether from syngas on the heterogeneous bifunctional hybrid catalysts. Appl Catal B. 2017; 217: 494-522.
25. Zhou W, Cheng K, Kang J, Zhou C, Subramanian V, Zhang Q, et al. New horizon in C1 chemistry: Breaking the selectivity limitation in transformation of syngas and hydrogenation of CO_2 into hydrocarbon chemicals and fuels. Chem Soc Rev. 2019; 48; 3193-3228.
26. Sierra I, Ereña J, Aguayo AT, Arandes JM, Bilbao J. Regeneration of $CuO\text{-}ZnO\text{-}Al_2O_3/\gamma\text{-}Al_2O_3$ catalyst in the direct synthesis of dimethyl ether. Appl Catal B. 2010; 94: 108-116.
27. Guinier A. Theorie et Technique de la Radiocristallographie. 2nd ed. Paris: Dunod; 1956. 736p.
28. Kipnis MA, Belostotskii IA, Volnina EA, Lin GI, Marshev II. Synthesis of dimethyl ether from syngas on the catalysts with the ZSM-5 zeolites. Kinet Catal. 2018; 59: 754-756.
29. Samokhin PV, Belostotskii IA, Marshev II, Kipnis MA. Chromatographic procedure for the determination of products of the direct synthesis of dimethyl ether. J Anal Chem. 2019; 74: S17-S23.
30. Simson G, Prasetyo E, Reiner S, Hinrichsen O. Continuous precipitation of $Cu/ZnO/Al_2O_3$ catalysts for methanol synthesis in microstructured reactors with alternative precipitating agents. Appl Catal A Gen. 2013; 450: 1-12.
31. Nakamoto K. Infrared and Raman spectra of inorganic and coordination compounds: Part A: Theory and applications in inorganic chemistry. New York: Wiley; 2009.
32. Kipnis MA, Belostotskii IA, Volnina EA, Lin GI. Synthesis of oxygenates from syngas on the $CuO/ZnO/Al_2O_3$ catalyst: The role of the dehydrating component. Catal Ind. 2019; 11: 53-58.

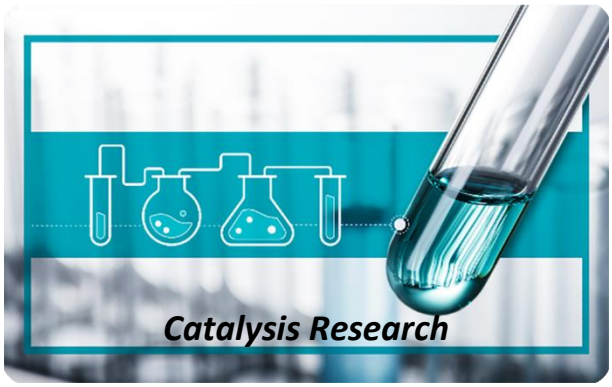

Enjoy *Catalysis Research* by:

1. Submitting a manuscript
2. Joining in volunteer reviewer bank
3. Joining Editorial Board
4. Guest editing a special issue

For more details, please visit:
http://www.lidsen.com/journals/cr